Macromolecular dynamics in crowded environments

Carlos Echeverria[1,2,a)] and Raymond Kapral[2,b)]
[1]*Laboratorio de Física Aplicada y Computacional, Universidad Nacional Experimental del Táchira, San Cristóbal 5001, Venezuela*
[2]*Department of Chemistry, Chemical Physics Theory Group, University of Toronto, Toronto, Ontario M5S 3H6, Canada*

(Received 21 October 2009; accepted 25 January 2010; published online 9 March 2010)

The structural and dynamical properties of macromolecules in confining or crowded environments are different from those in simple bulk liquids. In this paper, both the conformational and diffusional dynamics of globular polymers are studied in solutions containing fixed spherical obstacles. These properties are studied as a function of obstacle volume fraction and size, as well as polymer chain length. The results are obtained using a hybrid scheme that combines multiparticle collision dynamics of the solvent with molecular dynamics that includes the interactions among the polymer monomers and between the polymer beads and obstacles and solvent molecules. The dynamics accounts for hydrodynamic interactions among the polymer beads and intermolecular forces with the solvent molecules. We consider polymers in poor solvents where the polymer chain adopts a compact globular structure in solution. Our results show that the collapse of the polymer chain to a compact globular state is strongly influenced by the obstacle array. A nonmonotonic variation in the radius of gyration with time is observed and the collapse time scale is much longer than that in simple solutions without obstacles. Hydrodynamic interactions are important at low obstacle volume fractions but are screened at high volume fractions. The diffusion of the globular polymer chain among the obstacles is subdiffusive in character on intermediate time scales where the dynamics explores the local structure of the heterogeneous environment. For large polymer chains in systems with high obstacle volume fractions, the chain adopts bloblike conformations that arise from trapping of portions of the chain in voids among the obstacles. © *2010 American Institute of Physics*. [doi:10.1063/1.3319672]

I. INTRODUCTION

In living cells, polymers and other molecules carry out their biological functions in an aqueous environment containing microtubules and other filaments, various organelles and a variety of different macromolecular species and structural obstacles. In such systems, the macromolecular species and structural obstacles occupy a large volume fraction of the cell. The volume fraction often ranges from 0.1 to 0.4 of the total cellular volume.[1,2] Diffusion and reaction in such crowded and confined environments differ from those processes in a simple aqueous solution, and effects arising from crowding and confinement can influence biological function.[3,4]

Crowding and confinement in biological cells have been studied for many years.[5–8] It is known that they can alter equilibrium properties, such as equilibrium constants and molecular conformations.[8,9] They can also lead to substantial decreases in diffusion coefficients of macromolecules,[10–13] alter protein folding processes and influence protein assembly.[14–20]

There have been numerous studies of polymer dynamics in crowded environments and other disordered media using a variety of theoretical and simulation techniques and polymer models.[21,22] Various scaling regimes have been identified and scaling relations have been obtained that show how characteristic polymer static and dynamic properties depend on the degree of polymerization and crowding. Simulation studies have been carried out of continuous-space models of extended single polymer chains in the presence of obstacles (frozen networks of polymer chains or hard spherical obstacles).[23–27] Polymer structure and dynamics in crowded and confined systems is very different for long and short chains. Almost all simulation studies have been carried out without explicitly including solvent molecules in the description.

In this paper, we study the effects of molecular crowding on the structure and dynamics of macromolecules. While there have been many studies of polymers in random matrices, the effects of solvent quality on their behavior in such disordered systems has received less attention. The present investigations focus on polymers in poor solvents where the polymer chain adopts a compact globular form in the absence of crowding agents.[28] We consider dilute polymer solutions so that a single polymer chain may be studied. The polymer chain is solvated by a large number of solvent molecules and the solution contains fixed hard spherical obstacles that act as crowding agents.[29] In such systems, we examine the nature of the collapse of the polymer chain from an extended state to the equilibrium compact globular form,

[a)]Electronic mail: cecheve@unet.edu.ve.
[b)]Electronic mail: rkapral@chem.utoronto.ca.

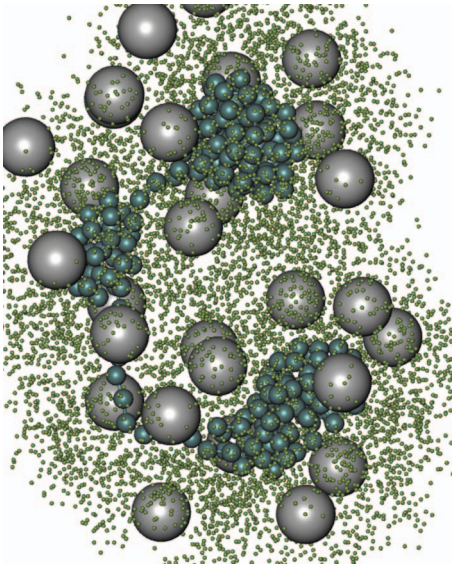

FIG. 1. An instantaneous configuration of the system showing the polymer chain and solvent containing obstacles. Only a portion of the system in the vicinity of the polymer chain is shown. The system parameters are the following: $N_b=200$, $\phi=0.25$, $R_o=2.0$, and $n_s=6$.

the changes in the equilibrium conformational structure of the polymer, and its translational diffusion as function of the degree of molecular crowding.

Full molecular dynamics (MD) simulations of systems containing a polymer, solvent and crowding obstacles require a large computational effort. In particular, the presence of a large number of solvent molecules, along with a large number of crowding agents, makes these calculations especially challenging. The explicit inclusion of solvent allows one to incorporate the effects solvent fluctuations and hydrodynamic interactions on polymer dynamics automatically, without having to specify approximate forms for the space-dependent friction tensor and random force in Brownian dynamics models. To overcome this difficulty, we employ a hybrid scheme that combines multiparticle collision (MPC) for the solvent[30–33] in conjunction with MD for the polymer molecule and its interactions with the solvent and obstacles. This allows us to investigate crowding effects on polymers in systems that include both solvent and crowding agents in a computationally efficient manner.

The outline of the paper is as follows. Section II describes the model system and presents details of the simulation method. In Sec. III, we discuss the effects of molecular crowding on polymer collapse dynamics, equilibrium polymer structure and translational diffusion. The conclusions of the study are presented in Sec. IV.

II. CROWDED SYSTEM

The crowded system we study comprises a single polymer molecule in a solution containing fixed hard spherical obstacles and solvent molecules (see Fig. 1). The total energy of the system is the sum of the kinetic energies of the polymer monomers and solvent molecules plus total potential energy $V(\mathbf{r}^{N_b},\mathbf{r}^{N_s},\mathbf{r}^{N_o})$, where N_b is the number of monomers (beads) in the polymer chain, N_s is the number of solvent molecules and N_o is the number of obstacles. We employ a hybrid dynamical model that combines a MD description of the polymer with a mesoscopic MPC dynamics for the solvent.[31] In this hybrid MD-MPC scheme, the total potential energy is the sum of the interactions among the polymer beads $V_{bb}(\mathbf{r}^{N_b})$, bead-solvent interactions $V_{bs}(\mathbf{r}^{N_b},\mathbf{r}^{N_s})$, as well as interactions between the fixed obstacles and monomer beads and solvent molecules, $V_{ob}(\mathbf{r}^{N_o},\mathbf{r}^{N_b})$ and $V_{os}(\mathbf{r}^{N_o},\mathbf{r}^{N_s})$, respectively. Interactions among the solvent molecules are accounted for by MPCs, described below. The number of obstacles N_o is an important parameter that controls the extent of crowding in the system. The specific forms of the interaction potentials among the components in the system are as follows.

Polymer bead-bead interactions. There are two types of interaction among the beads in our bead-spring model of a linear polymer chain. For neighboring beads, we use the non-Hookian finite extensible nonlinear elastic (FENE) interaction potential,[34,35]

$$V_{\mathrm{FENE}}(r)=-\frac{\kappa}{2}r_0^2\ln\left[1-\left(\frac{r}{r_0}\right)^2\right],\quad r<R, \tag{1}$$

where $\kappa=30\epsilon/\sigma$, ϵ is an energy parameter, σ is the bead diameter, $r=|\mathbf{r}_i-\mathbf{r}_j|$ is the distance between neighboring beads, and $r_0=1.5\sigma$ is its maximum value.

Non-neighboring beads interact through Lennard-Jones (LJ) potentials,

$$V_{\mathrm{LJ}}(r)=4\ \epsilon\left[\left(\frac{\sigma}{r}\right)^{12}-\left(\frac{\sigma}{r}\right)^{6}\right]. \tag{2}$$

The LJ potentials are cut off at a distance $L/4$, where L is the length of simulation box.

Polymer-solvent interactions. The solvent molecules interact with the polymer beads through repulsive LJ potentials,

$$V_{bs}(r)=\begin{cases}4\ \epsilon\left[\left(\frac{\sigma}{r}\right)^{12}-\left(\frac{\sigma}{r}\right)^{6}+\left(\frac{1}{4}\right)\right], & r\le 2^{1/6}\sigma\\ 0, & r>2^{1/6}\sigma,\end{cases} \tag{3}$$

which mimic hydrophobic interactions.

Obstacle-mobile particle interactions. The obstacles are taken to be hard spherical objects. They are randomly distributed in the system taking into account their excluded volume. The obstacle volume fraction is given by $\phi=4\ \pi N_o R_o^3/3\ \mathcal{V}$, where R_o is the obstacle radius and $\mathcal{V}$ is the volume of the system. When polymer beads or solvent particles collide with an obstacle, their velocities are reversed (bounce-back collisions).

Solvent-solvent interactions. There are no solvent-solvent interaction potentials. Instead, the effects of these interactions are accounted for by MPC dynamics.[30] In MPC dynamics, N_s solvent particles, representing coarse grained real molecules, stream and undergo effective collisions at discrete time intervals τ, accounting for the effects of many real collisions during this time interval. The collisions are carried out by dividing the system into a grid of cells with volumes $\mathcal{V}_\xi$ and assigning rotation operators $\hat{\omega}_\xi$, chosen from some set of rotation operators, to each cell of the system at

the time of collision. Particles within each cell "collide" with each other and the postcollision velocity of particle i in a cell ξ is given by $\mathbf{v}_i' = \mathbf{V}_\xi + \hat{\omega}_\xi(\mathbf{v}_i - \mathbf{V}_\xi)$, where $\mathbf{V}_\xi$ is the center of mass velocity of particles in the cell and $\hat{\omega}_\xi$ is the rotation operator of the cell ξ. The MPC dynamics satisfies mass, momentum, and energy conservation laws. The dynamics is microcanonical and preserves phase-space volumes.

A. Simulation details

To simulate the hybrid MD-MPC dynamics, Newton's equations of motion are solved to evolve the polymer and solvent, taking into account the forces derived from the bead-bead, bead-solvent, bead-obstacle, and solvent-obstacle interactions. Solvent-solvent forces do not enter in the Netwonian equations of motion. However, at time intervals τ, MPCs as described above take place and the evolution is continued. This hybrid dynamics again conserves mass momentum and energy and preserves phase space volumes.[30,31] There have been several studies of polymer dynamics in the absence of obstacles using MPC dynamics.[36–42]

The simulations presented in this paper were carried out on systems with volume $\mathcal{V}=L^3=(50)^3$ MPC cells with unit volume. The rotation operators in the MPC dynamics were chosen to describe rotations by $\alpha=\pm\pi/2$ about randomly chosen axes. The number of obstacles with radius R_o was computed from the desired value of the volume fraction ϕ. The obstacle radius R_o was varied from 2.0 to 5.0. The system also contains N_s mesoscopic solvent particles of mass $m=1$ (N_s varies from approximately 2.5×10^5 to 1.25×10^6) and one polymer with $N_b=40$, 60, 80, 100, 200, or 400 beads of mass $M=10m$ and diameter σ. The simulations were carried out in a cubic box with periodic boundary conditions. If the volume of a bead particle is $\mathcal{V}_b=\pi\sigma^3/6$ and the volume of an obstacle is $\mathcal{V}_o=4\ \pi R_o^3/3$, $\mathcal{V}_s$ is defined as the volume of the system occupied by solvent molecules, $\mathcal{V}_s=\mathcal{V}-N_b\mathcal{V}_b-N_o\mathcal{V}_o$. The MPC cell volume is given by $\mathcal{V}_\xi=\ell^3=1$. The average number density of solvent particles per cell $n_s=N_s/\mathcal{V}_s$ was varied but most simulation results are presented for $n_s=6$. The temperature was determined from the average kinetic energy and was taken to be $T=1/3$. The mesoscopic time was $\tau=0.5$. Thus, a particle moving with a velocity corresponding to the mean thermal velocity will travel on the order of one cell between MPCs. For parameter regimes where the particles travel on average a small fraction of a cell, random MPC grid shifting restores Galilean invariance.[43]

Dimensionless LJ units are used throughout the paper. Distances and energy are measured in units of σ and ϵ, respectively, time in units of $\sigma\sqrt{m/\epsilon}$, and temperature in units of ϵ/k_B. Newton's equations of motion were integrated using the velocity Verlet algorithm,[44] with a time step of $\Delta t=0.02\tau$.

III. EFFECTS OF CROWDING ON POLYMER STRUCTURE AND DYNAMICS

A. Polymer collapse

In a solution without obstacles, the polymers we study adopt compact globular structures and solvent molecules are excluded from the interiors of the globular polymers as a result of the hydrophobiclike bead-solvent interactions.[45] In this section, we study how the polymer collapse from an extended initial conformation to the globular form takes place when the environment is crowded by obstacles. Similar investigations of polymer collapse using MPC dynamics, including the role of hydrodynamic interactions on the collapse dynamics, have been carried out earlier.[41,42] In these studies, the polymer exchanges momentum with the solvent either by including the polymer beads in the MPC collision or by explicit bead-solvent interactions as in this study. These bead-solvent interactions capture some features of the solvent structure in the vicinity of the polymer chain; for example, they are able to account for the expulsion of solvent from collapsing chain and the resulting exclusion of solvent from the interior of our compact globular polymers. However, other aspects of the solvent structure, such as solvent structural order in the vicinity of the polymer chain that arises from solvent-solvent interactions are not described by this model.[46] To study the collapse in a solution that is crowded with randomly distributed obstacles, an extended configuration of a polymer chain was grown by adding monomers with bonds at random angles, consistent with exclusion by other monomers and obstacles. The time evolution of the polymer conformation from such initial states was monitored by computing the radius of gyration, $Rg(t)\equiv(N_b^{-1}\Sigma_{i=1}^{N_b}|(\mathbf{r}_i(t)-\mathbf{r}_P(t)\ |^2)^{1/2}$ as a function of the time t. Here, $\mathbf{r}_i(t)$ is the position of bead i and $\mathbf{r}_P(t)$ is the center mass position of the polymer at time t.

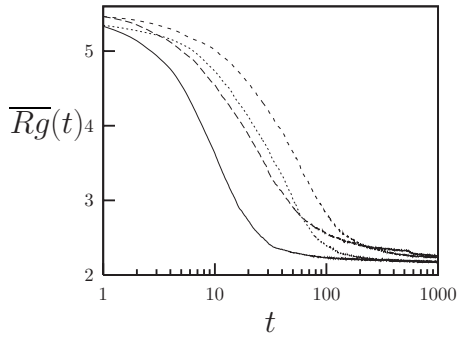

FIG. 2. Plots of the average radius gyration $\overline{Rg}(t)$ vs time on a semilogarithmic scale for a polymer with $N_b=100$ beads in a solvent with $n_s=6$ particles per cell computed from averages over 40–50 realizations of the dynamics. The effects of crowding and hydrodynamic interactions are investigated in this figure. The plot shows $\overline{Rg}(t)$ for MPC dynamics that includes hydrodynamic interactions with no obstacles (solid line), hydrodynamics and obstacles with $\phi=0.15$ (long dashed line), dynamics without hydrodynamic interactions (see text) and no obstacles (points line) and dynamics without hydrodynamic interactions, and obstacles with $\phi=0.15$ (short dashed line).

Figure 2, which presents plots of the radius of gyration averaged over realizations, $\overline{Rg}(t)$, as a function of time, shows the influence of crowding and hydrodynamic interactions on the collapse dynamics. As expected, the results in Fig. 2 show that the collapse time is longer in the presence of obstacles since, during collapse, the polymer must thread its way through the obstacles on the way to its final equilibrium state.

Hydrodynamic interactions are known to decrease the

TABLE I. The average collapse time τ_c with and without hydrodynamic interactions and different values of ϕ for a polymer with $N_b=100$ in a solvent with $n_s=6$ and obstacles with radius $R_o=2$.

ϕ	τ_c^H	τ_c^{nH}	$\tau_c^H/\tau_c^H(0)$	$\tau_c^{nH}/\tau_c^{nH}(0)$	τ_c^{nH}/τ_c^H
0.000	84	176	1.00	1.00	2.10
0.025	123	180	1.46	1.02	1.46
0.050	134	220	1.60	1.25	1.64
0.100	315	284	3.74	1.61	0.90
0.150	379	347	4.51	1.97	0.92
0.200	780	789	9.29	4.48	1.01

polymer collapse time. If hydrodynamic interactions are suppressed, each polymer bead acts as an independent source of friction; consequently, the frictional force on the polymer is much larger when hydrodynamic effects are neglected and the collapse occurs more slowly.[41,42] Hydrodynamic interactions may be eliminated in the simulations by replacing the stochastic rotation dynamics by random sampling of the postcollision velocities from a Boltzmann distribution. This random sampling destroys local momentum conservation and velocity correlations in the solvent which are responsible for hydrodynamic interactions. These considerations are borne out by the results in Fig. 2 where hydrodynamic interactions are suppressed. Although hydrodynamic interactions are expected to be screened by the presence of obstacles, we nevertheless see that for $\phi=0.15$, they still have a small noticeable influence on the collapse dynamics in the crowded system. For higher volume fractions, hydrodynamic interactions appear to be unimportant.

The definition of the average collapse time τ_c is somewhat arbitrary. Here we identify the collapse time as the time at which the ratio of the mean radius of gyration to its value at the initial time, both measured relative to the asymptotic value $\overline{Rg}$, takes a specific small fractional value f: $f=(\overline{Rg}(\tau_c)-\overline{Rg})/((\overline{Rg}(0)-\overline{Rg})$.[47] Taking $f=0.025$, the average collapse times, $\tau_c^H(\phi)$ or $\tau_c^{nH}(\phi)$, where the superscripts H or nH refer to dynamics with or without hydrodynamics, respectively, are shown in Table I. Various trends can be identified from an examination of the results in this table. For systems without obstacles, the collapse time is more that twice as long when hydrodynamic effects are neglected. As the volume fraction of obstacles increases the effects of hydrodynamic interactions decrease since these interactions are screened by obstacles. By volume fractions in the range of $\phi=0.1-0.2$ the results with and without hydrodynamic interactions are indistinguishable. (Even for the relatively large number of realizations used to obtain the results the ratio τ_c^{nH}/τ_c^H is difficult to estimate because the dynamics depends sensitively on the obstacle configuration for a realization.) Crowding produces very substantial increases in the collapse time.

These results depend strongly on the obstacle volume fraction and radius, and polymer size. The obstacle volume fraction and radius control the sizes of the voids in the obstacle array. For some values of the void size and polymer length, it may not be possible for a collapsed chain to occupy a single void, even if it could reach such a state. Figure 3, which compares the collapse dynamics for one realization in a crowded system with $\phi=0.1$ with that in a system with no obstacles, illustrates one of these features. For this realization of the dynamics, we see in the left inset in Fig. 3 that at intermediate times the polymer adopts a configuration with two globular domains; however, this configuration is not stable and the polymer continues to move among obstacles until it collapses to a nonspherical globular conformation (right inset). For this volume fraction and polymer length, it is still possible for the collapsed chain to occupy a single void, albeit with a somewhat distorted geometry.

B. Obstacles and polymer structure

Since both the volume fraction and radius of the obstacles control the structure and void sizes in the system, we now consider how these factors influence the equilibrium conformation of the collapsed polymer in the crowded system. Figure 4(a) plots $\overline{Rg}$ for a polymer with $N_b=100$ beads as function of volume fraction ϕ with $R_o=2.0$ and (b) is a plot of this quantity as function of the obstacle radius R_o for systems with a volume fraction of $\phi=0.3$. One of the features observed in previous studies of polymer conformations in crowded systems is the nonmonotonic variation in the polymer size with the obstacle volume fraction.[23,25,27,48] A similar trend is seen in Fig. 4(a) where $\overline{Rg}$ decreases slightly as ϕ increases from zero. Also, the fluctuations in Rg decrease in a small range of $\phi=[0.1,0.2]$. The globular configuration is compressed for small ϕ from its value at $\phi=0$. This is similar to what happens to a swollen polymer in a slightly crowded environment where $\overline{Rg}$ decreases.[25] In our

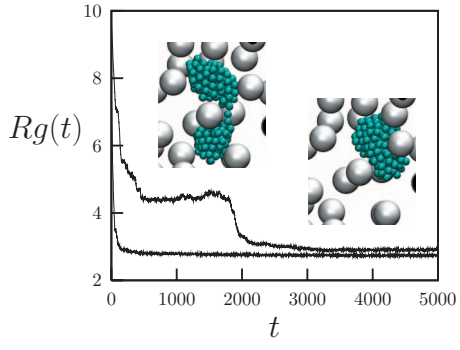

FIG. 3. Plots of the radius gyration $Rg(t)$ vs time t for a polymer with $N_b=200$ beads in a solvent with $n_s=6$ particles per cell. Results for two values of ϕ are shown: (bottom curve) $\phi=0.0$ and (top curve) $\phi=0.1$ with obstacles of radius $R_o=2.0$. The inset shows the polymer conformations in the presence of obstacles for $t<2000$ (left) and for $t>4000$ (right).

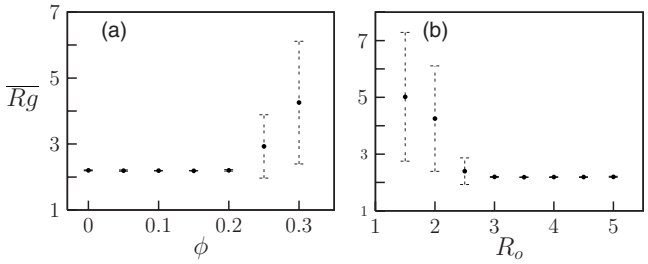

FIG. 4. (a) Average equilibrium radius gyration $\overline{Rg}$ vs ϕ for $R_o=2.0$ and (b) vs R_o for $\phi=0.3$. Solvent density is $n_s=6$. The error bars in this and the subsequent figures were estimated from eight realizations of the dynamics.

system this effect is very small since the equilibrium conformation for $\phi=0$ is already a tightly collapsed globular polymer.

For yet higher volume fractions, above $\phi\approx 0.2$ in the figure, the mean radius of gyration sharply increases. For these large volume fractions the final globular configuration has a nonspherical shape. The deformations of the globular conformations occur when the sizes of the cavities among the obstacles are less than the equilibrium radius gyration of the polymer. This effect is also seen in Fig. 4(b), where the variation in $\overline{Rg}$ with R_o is plotted for a fixed value of ϕ. As R_o decreases, the average void volume decreases and the polymer can no longer be accommodated in a void without considerable distortion.

As discussed above, polymer size can have a significant effect on these results since it may not be possible for a large polymer to occupy a single void. Figure 5 shows $\overline{Rg}$ as function of N_b on a logarithmic scale, with $\phi=0$ (filled circles), $\phi=0.1$ (open squares), $\phi=0.2$ (open circles), and $\phi=0.3$ (open triangles). For the solution without obstacles a simple scaling relation $\overline{Rg}\sim N_b^{\nu}$ is obtained. The exponent $\nu=0.34\pm0.03$ agrees with the theoretical value of 1/3 for a globular polymer. In the presence of obstacles this scaling relation is broken since the equilibrium conformations of sufficiently large polymers will be strongly distorted by the obstacle array. For such large polymers, the equilibrium conformation consists of several "bloblike" domains that are connected by short segments of the polymer chain.[23] This is shown in Fig. 6 for a polymer with $N_b=400$ in a medium with $\phi=0.2$. In this case, the voids in the system cannot

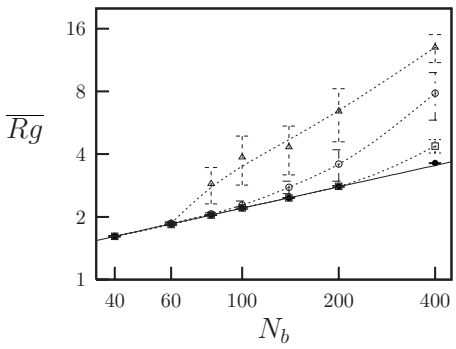

FIG. 5. The equilibrium radius gyration $\overline{Rg}$ as function of number of beads N_b in a log-log plot for an obstacle-free medium (filled circles; the solid line is fit to the data) and a medium containing obstacles with $R_o=2.0$ and $\phi=0.10$ (open squares), $\phi=0.20$ (open circles) and $\phi=0.30$ (open triangles). The dashed lines are guides to the eyes. The solvent density is $n_s=6$.

FIG. 6. The spatial configuration at time $t=1000$ for a polymer with $N_b=400$ beads in a medium with $\phi=0.3$, $R_o=2.0$, and $n_s=6$. Neither the obstacles nor the solvent molecules are shown in this visualization of the system.

accommodate the complete collapsed chain and five bloblike domains are formed in the conformation of polymer. The number of such domains, their sizes and their positions along the chain depend on the spatial configurations of obstacles and the initial polymer chain conformation. In such situations the equilibrium conformation of the polymer chain in the crowded system bears no resemblance to the simple globular form in the obstacle-free system. The conformations that the polymer adopts are largely controlled by the structure of the random obstacle array and solvent quality likely plays a minor role in determining the polymer structure. The diffusive dynamics in this regime also occurs by different mechanisms as discussed below.

C. Translational diffusion

The translation dynamics of polymers and biopolymers is strongly influenced by molecular crowding.[12] Both experiments and simulations indicate that large biopolymers may diffuse a few hundred times slower in highly crowded media than in aqueous solution. This situation should be contrasted with that of small molecules where diffusion coefficients decrease by only factors of roughly one half to one quarter as a result of crowding.[12,49]

Figure 7 shows the translational diffusion coefficient D as function of $(\overline{Rg})^{-1}$ for a system without obstacles. The radius of gyration was varied by changing the degree of polymerization, N_b. The diffusion coefficient was estimated from the slope of the mean square displacement (MSD) versus time t, $\mathrm{MSD}(t)=\langle|\mathbf{r}_P(t)-\mathbf{r}_P(0)|^2\rangle=6Dt$, where $\mathbf{r}_P$ is the center of mass of the globular polymer. The large, compact globular polymers considered here, where solvent is excluded from the interior of the polymer, can be considered as

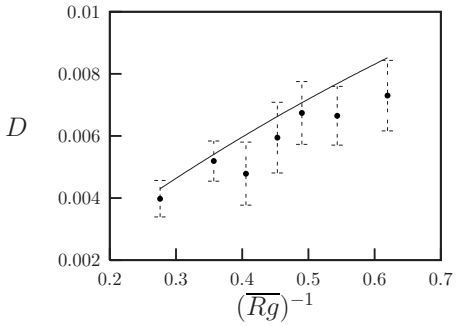

FIG. 7. Diffusion coefficient D vs $(\overline{Rg})^{-1}$ for a system without obstacles (solid circles). Solvent density is $n_s=6$.

rough spherical particles with radius R_P. In this case, the diffusion coefficient can be written as the sum of microscopic and hydrodynamic contributions,[50]

$$D = D_M + D_H = \frac{k_B T}{\zeta_M} + \frac{k_B T}{\zeta_H}, \tag{4}$$

where ζ is the friction coefficient and the subscripts M and H denote microscopic and hydrodynamic contributions, respectively. The microscopic friction arises from collisions of the solvent molecules with the surface monomers in the globular polymer and scales as $\zeta \sim R_P^2$, since the collision cross sections varies as the square of the polymer radius R_P. The kinetic theory approximation to ζ_M is

$$\zeta_M = \frac{8}{3} n_s R_P^2 (2\ \ \pi m k_B T)^{1/2}. \tag{5}$$

The hydrodynamic contribution arises from the coupling of the polymer to the solvent viscous modes and scales as $\zeta_H \sim R_P$. This contribution can be approximated by the Stokes friction coefficient for a sphere with radius R_P and stick boundary conditions: $\zeta_H = 6\ \pi \eta R_P$. For the collision rule used in this study, the viscosity of the mesoscopic solvent, η, that appears in this expression can be estimated from the formula $\eta = \eta^{\mathrm{kin}} + \eta^{\mathrm{col}}$, where the kinetic and collisional contributions to the viscosity are given by[43,51,52]

$$\eta^{\mathrm{kin}} = \frac{k_B T \tau \rho}{2m} \left(\frac{5\gamma - (\gamma - 1 + e^{-\gamma})(2 - \cos\alpha - \cos 2\alpha)}{(\gamma - 1 + e^{-\gamma})(2 - \cos\alpha - \cos 2\alpha)} \right), \tag{6}$$

and

$$\eta^{\mathrm{col}} = \frac{m}{18 a \tau} (\gamma - 1 + e^{-\gamma})(1 - \cos\alpha), \tag{7}$$

where γ_s is the average number of solvent molecules per collision cell and $\alpha = \pi/2$ is the MPC rotation angle. The effective polymer radius R_P in these equations is taken to be $R_P = \overline{Rg} + \sigma$ to account for the solvent-polymer bead repulsive interactions. The solid line is a plot of D determined from Eq. (4) with no additional fitting parameters, and it agrees quite well with the simulation results.

For the diffusion of small pointlike particles in a medium with obstacles, the effects of crowding on the diffusion coefficient for moderate obstacle volume fractions are well described[49] by the mean field expression,[53] $D(\phi) = D(\phi=0) \times (1-\phi)/(1+\phi/2)$. This formula, which describes the diffusion coefficient for point particles in a random array of hard obstacles that can move through arbitrarily small channels in the array, fails to describe the diffusion coefficient for the finite-size globular polymers studied here, which probe the sizes of the voids and channels in the array.

In a variety of random and heterogeneous media, diffusion is found to be anomalous[54,55] where the MSD is described by $\mathrm{MSD}(t) \sim t^{\alpha}$ with $\alpha \neq 1$. (The exponent α should not be confused with the MPC rotation angle introduced earlier.) In particular, subdiffusion where $\alpha < 1$ has been observed in the diffusion of proteins and finite-size probe particles in crowded cellular systems[56–59] and in membranes.[60,61] In random media with obstacles, anomalous diffusion is usually observed on characteristic spatial scales that depend on the obstacle volume fraction and obstacle size, both of which control the sizes of the voids and channels in medium, as well as the size of the diffusing particle. For short times that probe distances less than the characteristic spatial scale, normal diffusive behavior is seen, while subdiffusive behavior is observed in time domains that probe the characteristic spatial scales of the obstacle distribution. Provided system parameters are such that the particle does not become trapped, normal diffusion is again expected on long time scales.

In order to investigate the diffusive dynamics of the globular polymers when the system is crowded by obstacles, we computed the MSD for various values of the volume fraction, obstacle radius and polymer size. Due to system size and time scale constraints, our simulations are limited to intermediate times where the polymer is able to explore its local environment and is not confined to a single void. On this intermediate time scale, the diffusive dynamics of the globular polymers is found to be subdiffusive. However, the simulation time is too short to observe the crossover to normal diffusion at very long times[62] but the crossover from normal diffusion at short times to subdiffusion at intermediate times is seen. These results are shown in Fig. 8(a), which plots the MSD versus time on a log-log scale. The exponent α was determined by fitting the long time portion of the data to the power law form. The exponent α is found to depend on the volume fraction and decreases from unity (normal diffusion) when no obstacles are present to smaller values for nonzero ϕ indicative of subdiffusion in the presence of obstacles. Such dependence of α on the concentration of crowding agents has been observed in the subdiffusive dynamics in cells.[57–59]

The exponent α that characterizes subdiffusive behavior is also seen to depend on the obstacle radius R_o when the volume fraction is fixed [see Fig. 8(b)]. Both ϕ and R_o control the sizes of the voids and channels in the random array of obstacles. As R_o decreases for fixed ϕ, the characteristic void size decreases and the subdiffusive nature of the diffusive dynamics becomes more apparent. The inset in the figure shows that α decreases approximately linearly with R_o^{-1}.

The various spatial scales in a crowded system with fixed ϕ and R_o can also be probed by varying the size of the globular polymer. These results are presented in Fig. 8(c), which shows the MSD versus time for polymers with differ-

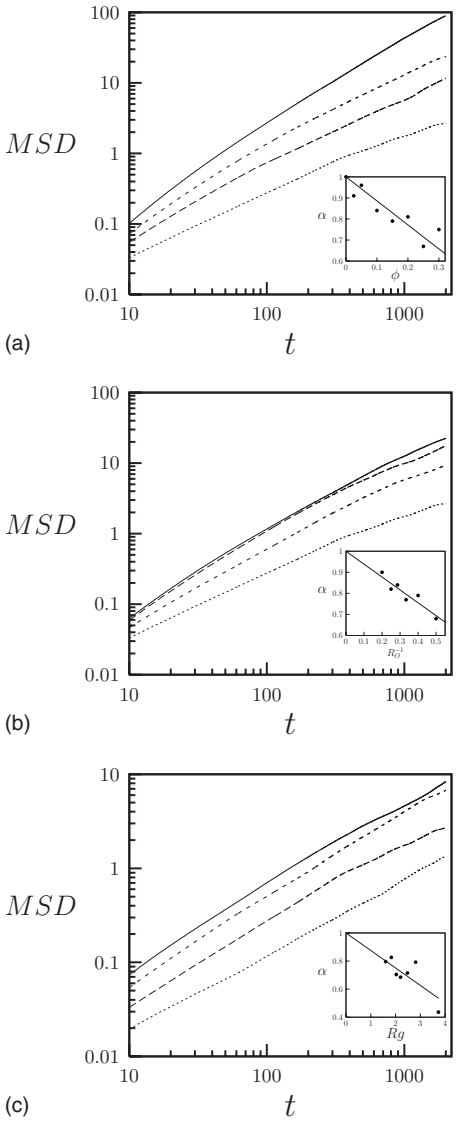

FIG. 8. (a) Log-log plot of the MSD(t) vs time: system with no obstacles (solid line); ϕ=0.025 (short dashed line); ϕ=0.050 (long dashed line) and ϕ=0.100 (points line). Obstacles have R_o=2, polymer size is N_b=100 and n_s=6. The inset shows the exponent α as a function of ϕ. (b) Log-log plot of the MSD vs time for various values of R_o with ϕ=0.1 and n_s=6: R_0=5 (solid line), R_0=4 (long dashed line), R_0=3 (short dashed line) and R_0=2 (points line). The inset shows the exponent α vs R_o^{-1}. (c) Variation of the MSD for various values of N_b for systems with ϕ=0.10, R_o=2, and n_s=6: N_b=40 (solid line), N_b=60 (short dashed line), N_b=100 (long dashed line)and N_b=200 (points line). The inset show the exponent α vs Rg.

ent numbers of beads. The inset plots α versus the average radius of gyration of the polymer. Although the estimates of α are subject to considerable uncertainty, it appears that α decreases as the polymer size increases.

The previous results for the MSD were for systems where the globular polymer could, on average, be accommodated in the voids in the random array. For long chains and high volume fractions as in Fig. 6, the collapsed polymer cannot fit, on average, into a single void, resulting in configurations like those shown in the figure. It is expected that the diffusive motions of such chains will occur by long time scale reptationlike motion but a full numerical exploration of this dynamics is a very lengthy task not considered in this study.

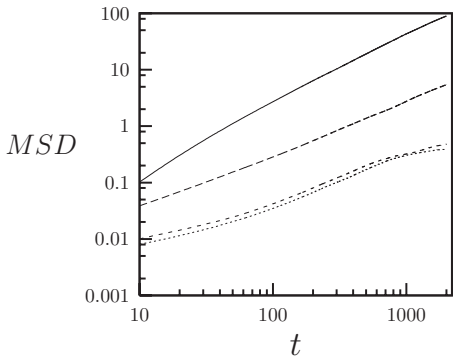

FIG. 9. Log-log plot of the MSD vs time for dynamics with hydrodynamic interactions and no obstacles (solid line), no hydrodynamic interactions and no obstacles (long dashed line), with hydrodynamic interactions and obstacles with ϕ=0.25 and R_o=2 (short dashed line) and no hydrodynamic interactions and obstacles with ϕ=0.25 and R_o=2 (points line). The solvent density is n_s=6 and N_b=100.

Finally, we consider the effects of hydrodynamic interactions on the MSD. Figure 9 shows the MSD versus time for systems with and without obstacles computed using MPC dynamics, which incorporates hydrodynamic interactions and dynamics where these interactions are suppressed. In these plots, we can see that, as expected and noted earlier for the collapse dynamics, hydrodynamic interactions are screened for large values of the volume fraction of obstacles.

IV. CONCLUSION

The results presented in this paper have provided quantitative information on how polymer dynamics and structure is changed by molecular crowding. Consistent with previous simulations on different models using other methods, we observed a nonmonotonic variation in the mean equilibrium radius of gyration with the volume fraction of obstacles and bloblike structures of long polymer chains that arise from trapping of portions of the chain in voids among the obstacles. The dynamical behavior of the crowded system not only depends on the volume fraction of obstacles but also on the obstacle radius and globular polymer size. This is expected in view of the fact that it is the fraction of the volume accessible to the diffusing polymers that plays an important role in the nature of the dynamics.[63]

The dynamics of the collapse to a globular state is strongly influenced by molecular crowding. Portions of long polymer chains become trapped in voids, as noted above, and this leads to nonmonotonic behavior in the variation in the radius of gyration with time and a much longer collapse time scale than in simple solutions without obstacles. The diffusion of the globular polymer chain among the obstacles is subdiffusive in character on the intermediate time scales and for the system sizes explored in our simulations. Simple mean field theories that are able to describe the variation in the diffusion coefficient with volume fraction for small pointlike molecules fail for large compact globular polymers in crowded systems.

Our results were obtained for a frozen random array of obstacles and observables were obtained from averages over the quenched disorder and dynamics. If the obstacles move then the trapped polymer configurations in systems with

quenched disorder will no longer occur and different dynamical behavior will be observed. If the time scale of this motion is long compared with other characteristic times in the system, our results will apply to this case provided times are restricted be much less that those for obstacle motion. Our simulation method can be extended easily to treat obstacle motion.

One of the distinctive features of the simulations carried out in this paper is the explicit inclusion of solvent in the model, albeit at a mesoscopic level. The interactions of the polymer beads with the solvent molecules were chosen to be repulsive, mimicking hydrophobic interactions, giving rise to a compact globular equilibrium polymer structure. Polymer and solvent interaction parameters may be chosen to mimic good solvents where the polymer chain exists in an expanded state in solution. In addition, because the solvent is included explicitly and MPC dynamics conserves momentum, hydrodynamic interactions are automatically incorporated in the description. Our simulation scheme can be used to study such systems as well as more complex crowding elements. Consequently, the results presented in this paper give additional insight into the effects of crowding on polymer structure and dynamics and provide a simulation framework in which to investigate crowding in more realistic models of physical and biological systems.

ACKNOWLEDGMENTS

This work was supported in part by a grant from the Natural Sciences and Engineering Research Council of Canada, Grant No. 5977–07. One of the authors (C.E.) acknowledges support from Decanato de Investigación, Universidad Nacional Experimental del Táchira, San Cristóbal, Venezuela.

[1] A. B. Fulton, Cell **30**, 345 (1982).
[2] T. M. Record, Jr., E. S. Courtenay, S. Caley, and S. J. Guttman, Trends Biochem. Sci. **23**, 190 (1998).
[3] D. S. Goodsell, Trends Biochem. Sci. **16**, 203 (1991).
[4] R. J. Ellis, Trends Biochem. Sci. **26**, 597 (2001).
[5] T. C. Laurent, Biophys. Chem. **57**, 7 (1995).
[6] S. P. Zimmerman and A. P. Minton, Annu. Rev. Biophys. Biomol. Struct. **22**, 27 (1993).
[7] A. P. Minton, J. Biol. Chem. **276**, 10577 (2001).
[8] H.-X. Zhou, G. Rivas, and A. P. Minton, Annu. Rev. Biophys. **37**, 375 (2008).
[9] N. A. Chebotareva, B. I. Kurganov, and N. B. Livanova, Biochemistry (Mosc.) **69**, 1239 (2004).
[10] K. Luby-Phelps, P. E. Castle, D. L. Taylor, and F. Lanni, Proc. Natl. Acad. Sci. U.S.A. **84**, 4910 (1987).
[11] N. D. Gershon, K. R. Porter, and B. L. Trus, Proc. Natl. Acad. Sci. U.S.A. **82**, 5030 (1985).
[12] A. S. Verkman, Trends Biochem. Sci. **27**, 27 (2002).
[13] M. Arrio-Dupont, G. Foucault, M. Vacher, P. F. Devaux, and S. Cribier, Biophys. J. **78**, 901 (2000).
[14] D. K. Eggers and J. S. Valentine, Protein Sci. **10**, 250 (2001).
[15] B. van den Berg, R. J. Ellis, and C. M. Dobson, EMBO J. **18**, 6927 (1999).
[16] R. J. Ellis and F.-U. Hartl, Curr. Opin. Struct. Biol. **9**, 102 (1999).
[17] S. B. Zimmerman and S. O. Trach, J. Mol. Biol. **222**, 599 (1991).
[18] H.-X. Zhou, J. Mol. Recognit. **17**, 368 (2004).
[19] L. Stagg, S.-Q. Zhang, M. S. Cheung, and P. Wittung-Stafshede, Proc. Natl. Acad. Sci. U.S.A. **104**, 18976 (2007).
[20] S.-Q. Zhang and M. S. Cheung, Nano Lett. **7**, 3438 (2007).
[21] A. Baumgärtner and M. Muthukumar, Adv. Chem. Phys. **94**, 625 (1996).
[22] *Statistics of Linear Polymers in Disordered Media*, edited by B. K. Chakrabarti (Elsevier, Amsterdam, 2005).
[23] V. Yamakov and A. Milchev, Phys. Rev. E **55**, 1704 (1997).
[24] S.-S. Chern and R. D. Coalson, J. Chem. Phys. **111**, 1778 (1999).
[25] A. Bhattacharya, J. Phys.: Condens. Matter **16**, S5203 (2004).
[26] R. Chang and A. Yethiraj, Phys. Rev. Lett. **96**, 107802 (2006).
[27] R. Chang and A. Yethiraj, J. Chem. Phys. **126**, 174906 (2007).
[28] The parameters that characterize the system can be changed to model polymers in good solvents.
[29] Various distinctions between crowding and confinement have been made in the literature. Crowding may refer to volume exclusion of one soluble macromolecule by another while confinement is anther type of crowding that arises from volume exclusion by a fixed confining boundary to a soluble macromolecule (Refs. 4 and 8). Other definitions refer to the volume exclusion effects from all fixed and molbile species as crowding (Ref. 12). Here, we adopt the more general terminology for crowding as volume exclusion effects arising from a distribution of accessible volumes in the system, even if the random obstacle array is fixed (Ref. 18).
[30] A. Malevanets and R. Kapral, J. Chem. Phys. **110**, 8605 (1999).
[31] A. Malevanets and R. Kapral, J. Chem. Phys. **112**, 7260 (2000).
[32] R. Kapral, Adv. Chem. Phys. **140**, 89 (2008).
[33] G. Gompper, T. Ihle, D. M. Kroll, and R. G. Winkler, Adv. Polym. Sci. **221**, 1 (2009).
[34] R. B. Bird, C. F. Curtiss, R. C. Armstrong, and O. Hassager, *Dynamics of Polymeric Liquids* (Wiley, New York, 1987).
[35] K. Kremer and G. Grest, J. Chem. Phys. **92**, 5057 (1990).
[36] M. Ripoll, K. Mussawisade, R. G. Winkler, and G. Gompper, Europhys. Lett. **68**, 106 (2004).
[37] R. G. Winkler, K. Mussawisade, M. Ripoll, and G. Gompper, J. Phys.: Condens. Matter **16**, S3941 (2004).
[38] R. G. Winkler, M. Ripoll, K. Mussawisade, and G. Gompper, Comput. Phys. Commun. **169**, 326 (2005).
[39] K. Mussawisade, M. Ripoll, R. G. Winkler, and G. Gompper, J. Chem. Phys. **123**, 144905 (2005).
[40] A. Malevanets and J. M. Yeomans, Europhys. Lett. **52**, 231 (2000).
[41] I. Ali, D. Marenduzzo, and J. M. Yeomans, J. Chem. Phys. **121**, 8635 (2004).
[42] S. H. Lee and R. Kapral, J. Chem. Phys. **124**, 214901 (2006).
[43] T. Ihle and D. M. Kroll, Phys. Rev. E **63**, 020201 (2001).
[44] D. Frenkel and B. Smit, *Understanding Molecular Simulation: From Algorithms to Applications* (Academic, New York, 1996).
[45] These results were confirmed by computations of the radial distribution function for solvent molecules relative to the center of mass of the compact globular chain.
[46] R. Chang and A. Yethiraj, J. Chem. Phys. **114**, 7688 (2001) (and references therein).
[47] N. Kikuchi, A. Gent, and J. M. Yeomans, Eur. Phys. J. E **9**, 63 (2002).
[48] G. W. Slater and G. I. Nixon, J. Chem. Phys. **108**, 3310 (1998).
[49] C. Echevería, K. Tucci, and R. Kapral, J. Phys.: Condens. Matter **19**, 065146 (2007).
[50] J. T. Hynes, R. Kapral, and M. Weinberg, J. Chem. Phys. **70**, 1456 (1979).
[51] A. Lamura, G. Gompper, T. Ihle, and D. M. Kroll, Europhys. Lett. **56**, 319 (2001).
[52] N. Kikuchi, C. M. Pooley, J. F. Ryder, and J. M. Yeomans, J. Chem. Phys. **119**, 6388 (2003).
[53] J. Lebenhaft and R. Kapral, J. Stat. Phys. **20**, 25 (1979).
[54] S. Havlin and D. Ben-Avraham, Adv. Phys. **36**, 695 (1987).
[55] R. Metzler and J. Klafter, Phys. Rep. **339**, 1 (2000).
[56] M. Wachsmuth, W. Waldemar, and J. Langowski, J. Mol. Biol. **298**, 677 (2000).
[57] M. Weiss, M. Elsner, F. Kartberg, and T. Nilsson, Biophys. J. **87**, 3518 (2004).
[58] D. S. Banks and C. Fradin, Biophys. J. **89**, 2960 (2005).
[59] G. Guigas, C. Kalla, and M. Weiss, Biophys. J. **93**, 316 (2007).
[60] G. Schutz, H. Schindler, and T. Schmidt, Biophys. J. **73**, 1073 (1997).

[61] M. Weiss, H. Hashimoto, and T. Nilsson, Biophys. J. **84**, 4043 (2003).
[62] For the volume fractions and obstacle and polymer sizes we consider the globular polymer can explore the heterogeneous medium and normal diffusion will be observed, but on time scales longer than our simulation times. In addition, we note that, while our globular polymers are compact, they are composed of a chain of beads and can deform during their diffusive dynamics in the array of obstacles. Thus, obstacle configurations that might block the diffusion a globular polymer when treated as a hard spherical object, will not do so when the polymer can be deformed. This very long time diffusive domain has not been explored in our simulations.
[63] S. Babu, J. C. Gimel, and T. Nicolai, J. Phys. Chem. B **112**, 743 (2008).